

Learning-Based Rich Feedback HARQ for Energy-Efficient Uplink Short Packet Transmission

Martin V. Vejling^{*}, Federico Chiariotti[†], Anders E. Kalør[‡], Deniz Gündüz[§], Gianluigi Liva[¶], Petar Popovski^{*}

^{*}Dept. of Electronic Systems, Aalborg University, Denmark ({mvv,petarp}@es.aau.dk)

[†]Dept. of Information Engineering, University of Padova, Italy (chiariot@dei.unipd.it)

[‡]Dept. of Information and Computer Science, Keio University, Japan (aek@keio.jp)

[§]Dept. of Electrical and Electronic Engineering, Imperial College London, UK (d.gunduz@imperial.ac.uk)

[¶]Inst. of Communications and Navigation, German Aerospace Center (DLR), Wessling, Germany (gianluigi.liva@dlr.de)

Abstract—The trade-off between reliability, latency, and energy efficiency is a central problem in communication systems. Advanced hybrid automated repeat request (HARQ) techniques reduce retransmissions required for reliable communication but incur high computational costs. Strict energy constraints apply mainly to devices, while the access point receiving their packets is usually connected to the electrical grid. Therefore, moving the computational complexity from the transmitter to the receiver may provide a way to improve this trade-off. We propose the reinforcement-based adaptive feedback (RAF) scheme, a departure from traditional single-bit feedback HARQ, introducing adaptive *rich feedback* where the receiver requests the coded retransmission of specific symbols. Simulation results show that RAF achieves a better trade-off between energy efficiency, reliability, and latency, compared to existing HARQ solutions. Our RAF scheme can easily adapt to different modulation schemes and can also generalize to different channel statistics.

Index Terms—Rich feedback, HARQ, energy efficiency, short codes.

I. INTRODUCTION

Over the past few years, Internet of Things (IoT) systems have become ubiquitous: factories, buildings, farms, and urban environments now have extensive networks of simple IoT devices, which are used to collect all sorts of data, improving energy efficiency and informing economic and policy decisions [1], [2]. Most IoT devices have very long design lifespans, often measured in years or decades [3], and thus their main limitation is the energy consumption, since replacing batteries is an expensive operation in many cases. As a result, energy efficiency is a significant concern in IoT research, and several low-energy protocols have been developed [4].

In addition to the energy consumption, IoT devices are typically characterized by short packet transmissions, primarily in the uplink [2]. Furthermore, some applications, such as industrial and environmental monitoring, require relatively high reliability. To achieve this, IoT devices typically implement retransmission schemes such as hybrid automated

repeat request (HARQ) [5], in which the receiver combines all previous transmissions to decode a message. As such, HARQ dynamically adjusts the transmission rate to the instantaneous channel conditions. While extra transmissions come at the cost of increased delay and energy consumption at the device, only retransmitting information when it is necessary contributes to an average reduction in the total energy consumption.

Overall, HARQ introduces a fundamental trade-off between reliability, latency, and energy consumption: (i), a low coding rate in the first transmission leads to fewer rounds of HARQ, and hence a lower latency, but requires more energy; (ii), transmitting few symbols in each round leads to higher latency and lower reliability, but is more energy efficient, as the energy-constrained device transmits the exact number of symbols needed to decode the message [6]. On the other hand, multiple rounds of feedback can also lead to a high energy consumption, as the reception of the feedback may require almost as much energy as active transmission [7]. Computation is another aspect that cannot be neglected: complex schemes that put a significant computational load on the transmitter side can deplete batteries just as quickly as inefficient transmission [8].

In this paper, we propose a new HARQ strategy, termed reinforcement-based adaptive feedback (RAF), designed to minimize the total energy consumption of a device transmitting in the uplink while maintaining a relatively low latency and high reliability. The main idea behind RAF is to move the complexity from the transmitter to the receiver, which does not have the same energy limitations, and to adaptively and optimally exploit reliability-based HARQ (RB-HARQ) [9] by informing the transmitter exactly which parts of the packet are the most ambiguous. This way, the transmitter can construct retransmissions that directly target these portions of the packet, thereby increasing the likelihood that the retransmission will contribute to correct decoding of the message, while keeping the complexity at the device low.

The main contributions can be summarized as follows:

- 1) We propose RAF, an RB-HARQ scheme, which learns the optimal mapping of the posterior probabilities, obtained from the belief propagation (BP) decoder, to the list of symbols for retransmission. Since the complex

This work was partly funded by the Villum Investigator Grant “WATER” financed by the Villum Foundation, Denmark. The work of F. Chiariotti was financed by the European Union under the Italian National Recovery and Resilience Plan of NextGenerationEU, under the “SoE Young Researchers” grant REDIAL (SoE0000009). The work of A. E. Kalør was supported by the Independent Research Fund Denmark (IRFD) under Grant 1056-00006B.

interaction between the encoder and decoder of such a code makes it hard to describe the feedback policy analytically, we model the feedback design problem as a Markov decision process (MDP), and use deep reinforcement learning (DRL) to optimize the trade-off between the energy efficiency and latency while guaranteeing high reliability.

- 2) The proposed scheme is compared to existing HARQ, dynamic HARQ (D-HARQ), and RB-HARQ solutions in the context of multiplicatively repeated (MR) non-binary low-density parity check (LDPC) codes with different modulation schemes and channels.

Our simulations show that RAF can outperform the existing HARQ, D-HARQ, and RB-HARQ policies by improving all key performance indicators (KPIs) simultaneously. Specifically, with an additive white Gaussian noise (AWGN) channel, we are able to reduce the undetected error rate by a factor of 4, while latency is decreased by 4% and energy efficiency is increased by 1% with respect to the optimized benchmarks. For a block fading channel, energy efficiency improves by up to 4% with the same latency.

The rest of this paper is organized as follows. Sec. II introduces the system model, including the energy model, and the HARQ scheme considered in this work. Sec. III then presents the proposed RAF scheme, describing the MDP formulation and the adopted deep Q-network (DQN) approach. Numerical results are presented in Sec. IV, and Sec. V concludes the paper and presents some future research directions.

II. SYSTEM MODEL

We consider an energy-constrained device transmitting a K -bit message $m \in \{0, 1, \dots, 2^K - 1\}$ in the uplink to a base station over a wireless channel with minimal energy usage, high reliability, and low latency. The receiver has a relaxed energy constraint and high computational capabilities. Transmission occurs in rounds $t = 0, 1, \dots, T_{\max} - 1$, involving uplink data transmission of a variable number of code symbols L_t over \hat{L}_t channel uses, and a fixed number of downlink feedback symbols L_f over \hat{L}_f channel uses. For instance, with M -ary quadrature amplitude modulation (QAM) and codewords over the order- q Galois field (GF) \mathbb{F}_q , the number of uplink channel uses in the t -th round is $\hat{L}_t = \frac{\log_2(q)}{\log_2(M)} L_t$, and the communication rate after the t -th round is $R_t = K / (\sum_{i=0}^t \hat{L}_i)$ bits per channel use. We will assume that $q \leq M$ so that each code symbol produces $\frac{\log_2(q)}{\log_2(M)} \geq 1$ channel symbols, but the general framework can be applied to the alternative case as well. The same modulation scheme is used for downlink, so that $\hat{L}_f = \frac{\log_2(q)}{\log_2(M)} L_f$. To facilitate channel estimation, each frame (both uplink and downlink) also contains a preamble of \hat{L}_p channel uses.

Uplink symbols $\mathbf{x}_t \in \mathbb{C}^{\hat{L}_t}$ have normalized power and are transmitted over a block fading channel, yielding received signals $\mathbf{y}_t = \beta_t \mathbf{x}_t + \mathbf{w}_t$, where $\beta_t \stackrel{iid}{\sim} P_\beta$ is the instantaneous fading coefficient independent and identically distributed (iid.) from some distribution P_β , and $\mathbf{w}_t \sim \mathcal{CN}(\mathbf{0}, \sigma^2 \mathbf{I})$ is AWGN.

The instantaneous signal to noise ratio (SNR) is given by $\text{SNR}_t = \frac{|\beta_t|^2}{\sigma^2}$. Feedback is assumed to be error-free since the receiver can transmit at a much higher power, but feedback errors can be accounted for within the MDP formulation.

A. Energy Model

We assume that, on average, transmitting and receiving a single symbol requires energy of P_s and P_f , respectively. The precise values of P_s and P_f depend on the physical implementation of the communication system and encompasses energy consumption of active radio frequency (RF) chains as well as encoding and decoding operations. We parameterize $P_f = \alpha P_s$, where $\alpha \in [0, 1]$ models the relative energy expenditure of receiving feedback compared to transmitting (we assume that $P_f \leq P_s$, as in most practical systems).

With this in mind, the average energy spent by the device in the t -th round is $E(t) = P_s(\hat{L}_p + \hat{L}_t) + \alpha P_s(\hat{L}_p + \hat{L}_t)$, and the average cumulative energy consumed up until and including the t -th round is $E_{\text{tot}}(t) = \sum_{i=0}^t E(i)$. We further denote the number of successful information bits transmitted per energy unit as $E_b(t) = \frac{K}{E_{\text{tot}}(t)} \mathbb{1}[\hat{\mathbf{c}}_t = \mathbf{c}]$, where $\mathbb{1}[\cdot]$ is the indicator function, equal to 1 if the condition is true, and 0 otherwise, and $\hat{\mathbf{c}}_t$ is the decoder's estimate of \mathbf{c} .

B. HARQ Scheme

In the first round, $t = 0$, message m is encoded into an initial codeword $\mathbf{c} \in \mathcal{C}$ of L_0 code symbols, which is mapped to \hat{L}_0 channel symbols, and transmitted along with the preamble. In subsequent rounds, the transmitter constructs *additional* L_0 code symbols, punctures them to $L_t \leq L_0$ symbols, and transmits the \hat{L}_t channel symbols along with the preamble. The puncturing pattern is denoted $\mathbf{f}_t \in \{0, 1\}^{L_0}$ with a 1 in the i -th entry indicating the transmission of the i -th symbol, such that $L_t = \sum_{i=1}^{L_0} \mathbf{f}_t(i) \leq L_0$. This continues until either the receiver is able to decode the message and the device receives an ACK, or a maximum of T_{\max} rounds are completed.

The decoder employs BP decoding with at most I BP iterations to obtain an estimate $\hat{\mathbf{c}}_t$ of \mathbf{c} based on the received signals $\mathbf{y}_0, \dots, \mathbf{y}_t$. The BP decoder takes the SNR as input, and for simplicity, we will assume that the SNR is perfectly estimated using the preamble symbols. However, note that BP decoders, such as the one used in this work, generally perform well even with imperfect estimates [10]. If $\hat{\mathbf{c}}_t$ is a valid codeword, i.e., $\hat{\mathbf{c}}_t \in \mathcal{C}$, the message is assumed to be correctly received and the receiver terminates the transmission by sending an ACK. On the other hand, if $\hat{\mathbf{c}}_t$ is not a valid codeword, then the receiver transmits a NACK and a feedback signal (unless $t = T_{\max} - 1$, in which case the transmission is abandoned and the message is dropped).

The outlined HARQ scheme can be employed with any rate adaptive code allowing for soft decoding, including polar codes, turbo codes, and more. However, in this work, we limit our attention to MR non-binary LDPC codes [11], as these have proven to be efficient for short packet transmissions [12].

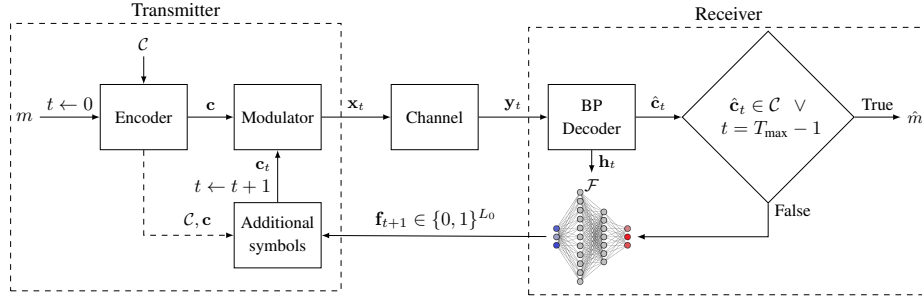


Fig. 1. Block diagram of the proposed rich feedback protocol, RAF.

III. REINFORCEMENT-BASED ADAPTIVE FEEDBACK

In this section, we present our proposed adaptive feedback scheme. We first introduce the general feedback design, and then show how to learn the feedback policy using DRL. We propose to control the transmissions by providing a puncturing pattern in the feedback link. Specifically, in round t we provide $\mathbf{f}_{t+1} \in \{0, 1\}^{L_0}$, indicating the binary puncturing pattern that should be used for the uplink transmission in round $t+1$. As a result, the uncoded feedback message has length L_0 , and consequently $L_t = \lceil \frac{L_0}{\log_2 q} \rceil^1$.

The objective is to learn a policy that chooses the optimal puncturing pattern by using the information from previous rounds, represented by the a posteriori probabilities estimated by the BP decoder, which are denoted by the matrix $\mathbf{P}_t = [\Pr(s_i = \zeta_j | \mathbf{y}_t, \dots, \mathbf{y}_0)]_{ij}$ where ζ_j is the j -th element in the GF \mathbb{F}_q . We make the simplification to only consider the a posteriori entropy vector, $\mathbf{h}_t \in \mathcal{S} = [0, \log_2 q]^{L_0}$, of the code symbols s_i , $i = 1, 2, \dots, L_0$, of the code \mathcal{C} , defined as

$$\mathbf{h}_t(i) = - \sum_{j=0}^{q-1} [\mathbf{P}_t]_{ij} \log_2 [\mathbf{P}_t]_{ij}. \quad (1)$$

The choice of using \mathbf{h}_t as the state, as opposed to the full code symbol probability matrix \mathbf{P}_t , is justified by empirical results indicating that using \mathbf{P}_t does not lead to improvements in the results. The feedback message in round t is then constructed as $\mathbf{f}_{t+1} = \mathcal{F}(\mathbf{h}_t)$, where $\mathcal{F} : \mathcal{S} \rightarrow \{0, 1\}^{L_0}$ is a deterministic function that maps the entropy vector to a message of L_0 bits indicating the puncturing pattern to be used in round $t+1$. We formulate the objective as

$$\mathcal{F}^* = \arg \max_{\mathcal{F} : \mathcal{S} \rightarrow \{0, 1\}^{L_0}} \mathbb{E}_{\mathcal{F}} [E_b(T) \gamma^T], \quad (2)$$

where $\mathbb{E}_{\mathcal{F}}$ is the expected value operator given that the agent follows policy \mathcal{F} , T is the number of transmission rounds until termination, and $\gamma \in (0, 1]$ is an exponential discount factor that is meant to ensure low latency (lower values of γ lead the system to prioritize latency over energy efficiency). The expectation in Eq. (2) is over \mathbf{c} , generated from encoding a message m drawn uniformly from the set of messages, and T which given \mathcal{F} and \mathbf{c} depends only on the

¹For simplicity, we assume no encoding or compression of the puncturing pattern, noting that the flexibility in the energy model keeps the presentation general.

channel realizations. For simplicity, we restrict our attention to stationary, deterministic policies. The proposed rich feedback communication protocol is summarized in Fig. 1.

A. MDP Formulation

The problem introduced in Eq. (2) is approximated by an MDP assuming that the next entropy vector is approximately independent of the past given the chosen action and the current entropy vector.² Under this assumption, the MDP policy amounts to repeatedly applying \mathcal{F} to the current state \mathbf{h}_t , followed by receiving a *reward* r_t . The optimal function \mathcal{F}^* can be found using reinforcement learning (RL) techniques, such as policy evaluation, policy iteration, value iteration, Q-learning, etc. [13]. In this work, we consider Q-learning with the purpose of exploiting the well-known DQN approach [14].

The number of actions in the proposed MDP is 2^{L_0} . To simplify, we instead consider selecting the *number* of symbols to be retransmitted in the next round, and denote this policy as $\tilde{\mathcal{F}} : \mathcal{S} \rightarrow \mathcal{A}$, where $\mathcal{A} = \{1, \dots, L_0\}$ is the action space of the MDP (the action of requesting zero symbols is selected automatically if $\hat{\mathbf{c}}_t \in \mathcal{C}$). The symbols to be retransmitted are then requested deterministically as the ones with the highest entropy computed using Eq. (1), i.e.,

$$[\mathcal{F}(\mathbf{h}_t)]_i = 1 \left[\sum_{j \neq i} \mathbb{1}[\mathbf{h}_t(i) < \mathbf{h}_t(j)] < \tilde{\mathcal{F}}(\mathbf{h}_t) \right], \quad (3)$$

where $\tilde{\mathcal{F}}(\mathbf{h}_t)$ is the number of symbols to be transmitted. The simplification above is justified by empirical results that suggest optimizing an agent to select which symbols to retransmit yields no performance gains compared to selecting the maximum entropy symbols.

Due to the episodic nature of the MDP, we set rewards $r_t = 0$ for $t = 1, \dots, T-1$, and only assign non-zero rewards at the end of a transmission (episode). With this structure, the final MDP is defined as finding $\tilde{\mathcal{F}}^*$ that solves

$$\tilde{\mathcal{F}}^* = \arg \max_{\tilde{\mathcal{F}} : \mathcal{S} \rightarrow \mathcal{A}} \mathbb{E}_{\mathcal{F}} [r_T \gamma^T], \quad (4)$$

where r_T is the reward for the end of the episode. While $E_b(T)$ would be a natural choice for rewards, we have empirically

²This is only an approximation, since the posterior probabilities do not exactly satisfy the Markov property even though the channel realizations are independent.

observed faster convergence and more robust training across simulation settings by defining the reward as

$$r_T = (2 \cdot \mathbb{1}[\hat{\mathbf{c}}_T = \mathbf{c}] - 1) - \frac{E_{\text{tot}}(T)}{\mathbb{E}_{\mathcal{F}_0}[E_{\text{tot}}(T)]}, \quad (5)$$

where \mathcal{F}_0 is a naïve static policy taking actions $L_t = 1, \forall t > 0$, and is included as it provided improvements in convergence of the learning algorithm. We have that, $\mathbb{E}_{\mathcal{F}_0}[E_{\text{tot}}(T)] = \mathbb{E}_{\mathcal{F}_0}[T]P_s(\hat{L}_p(1+\alpha) + \alpha\hat{L}_f + 1) + P_s(\hat{L}_p(1+\alpha) + \alpha\hat{L}_f + \hat{L}_0)$. Now, by simulating episodes using the naïve static policy, we can approximate $\mathbb{E}_{\mathcal{F}_0}[T]$ by the average number of rounds, and in turn approximate $\mathbb{E}_{\mathcal{F}_0}[E_{\text{tot}}(T)]$.

As mentioned, we will use Q-learning to solve this MDP. In Q-learning, the objective is to use observations of the environment to learn an *action-value* function, $Q(\mathbf{h}, a)$, that characterizes the expected long-term reward of taking action a in state \mathbf{h} . Given the estimated action-value function and a state, \mathbf{h}_t , the action is selected as $a_t = \arg \max_{a \in \mathcal{A}} Q(\mathbf{h}_t, a)$.

The state transitions in the MDP are complex, as they depend both on the transmission of the new code symbols and the BP decoder, so we cannot model them analytically. Additionally, since $\mathcal{S} = [0, \log_2 q]^{L_0}$, the state space is infinite, so using a lookup table would not be feasible [15]. Instead, we consider the DQN approach [14], which uses a neural network to approximate the value function.

B. Deep Q-Learning

The DQN takes the entropy vector \mathbf{h}_t as input, and returns an estimate of $Q(\mathbf{h}_t, a_t), \forall a_t \in \mathcal{A}$. We employ a fully connected deep neural network using rectified linear unit (ReLU) activation functions with number of layers and number of hidden units in the respective layers expressed by the tuple N_{hidden} , and L_0 output units.

For training, we adopt replay memory [14] where agent experience is stored in tuples $e_t = (\mathbf{h}_t, a_t, r_t, \mathbf{h}_{t+1})$. The replay memory buffer size is denoted by MEM, and as new experience samples are observed the oldest experience is deleted from the replay memory buffer. During training, batches of size BS are sampled from the replay memory in order to optimize the neural network parameters using backpropagation with the ADAM algorithm and gradient clipping with max gradient norm, GC. The number of episodes between training sessions is F_{upd} and the number of parameter updating steps per training session is N_{upd} .

Moreover, as in [14], to avoid biases, two different Q functions, denoted by Q_A and Q_B , are used to select and evaluate actions, respectively. The model is updated by

$$Q_A^{\text{new}}(\mathbf{h}_t, a_t) = (1 - \eta)Q_A(\mathbf{h}_t, a_t) + \eta(r_t + \gamma_{\text{DQN}} \max_{a_{t+1} \in \mathcal{A}} Q_B(\mathbf{h}_{t+1}, a_{t+1})), \quad (6)$$

where η is the learning rate and γ_{DQN} is the DQN discount factor. When $\gamma_{\text{DQN}} = 0$, the agent will strive to achieve immediate rewards while when $\gamma_{\text{DQN}} = 1$, the agent evaluates the actions based on the sum total of the future rewards. The parameters of Q_B are then updated by copying the parameters of Q_A after every F_{mod} training sessions.

TABLE I
SCENARIO AND DQN SETTINGS

Parameter	Value	Description	Parameter	Value	Description
K	40 bits	Payload size	L_0	15 symbols	Codeword length
q	256	Galois field order	SNR	6 dB	Received SNR
I	5	Max BP iterations	E_{first}	0.6 mJ	Energy reference [16]
τ_p	1 ms	Packet slot duration	$\mathbb{E}_{\mathcal{F}_0}[T]$	7.7	Normalization factor
T_{max}	15	Max rounds	η	0.001	Learning rate
BS	64	Batch size	F_{upd}	100	Training frequency
GC	5	Max gradient norm	MEM	60000	Memory replay buffer
N_{upd}	15	Training steps per update	N_{hidden}	[64, 32, 16]	Hidden layer sizes
F_{mod}	10	Target update frequency	ε_d	0.05	Exploration decay rate
ε_0	1	Initial exploration rate	F_ε	8000	Exploration decay freq.
ε_{min}	0.4	Min exploration rate	N_{test}	300000	Test episodes
N_{train}	270000	Training episodes			

During experience gathering, the agent uses the ε -greedy policy. The ε -greedy parameter is initialized as ε_0 and decreases linearly with a decay parameter ε_d every F_ε simulated episodes, with a minimum preset as ε_{min} .

IV. SIMULATION SETTINGS AND RESULTS

We define a scenario corresponding to the one given in Sec. III, with a transmitter encoding packets containing $K = 40$ bits of information into $L_0 = 15$ symbols using a codebook of order $q = 256$, i.e., with code rate $1/3$. The transmitter employs MR non-binary LDPC codes [17], defined over \mathbb{F}_q , which allows the device to generate codes with successively lower rates by concatenating previous codewords with a new set of symbols. In the following, we will consider a modulation order of $M = 256$ unless otherwise stated. Although this setting is more suitable for complex applications than for IoT [18], it simplifies the presentation: with this value, each code symbol maps exactly to one constellation point, i.e., $\hat{L}_t = L_t$. We will also show results for quadrature phase-shift keying (QPSK) ($M = 4$) below. We consider four baseline policies as benchmarks:

- 1) *HARQ*: we fix L_t to a constant for each $t > 0$ and use a random uniform symbol selection policy to select L_t different symbols. This policy only requires 1 bit of feedback as with traditional HARQ. We set $L_f = 1$.
- 2) *D-HARQ*: we adaptively determine L_t as the number of symbols that have an entropy higher than a given threshold value H_{th} . This is an adaptation of the ideas in [19] to the present scenario. It requires 4 bits of feedback and we set $L_f = 1$.
- 3) *Static tapered (ST) HARQ*: we fix L_t to a constant for each $t > 0$. Unlike the HARQ and D-HARQ policies, this policy selects the maximum entropy symbols, and is an adaptation of the ideas in [9] to the present scenario. The full 15 bit feedback is required, and we set $L_f = 2$.
- 4) *Threshold-based adaptive (TA) HARQ*: this policy selects for retransmission all the symbols that have an entropy higher than a given threshold value H_{th} , and is based on the ideas in [20]. It requires the full 15 bit feedback. Again, we set $L_f = 2$.

In this study, for $L_p = 0$ the energy cost of the first round is fixed as $E_{\text{first}} = 0.6$ mJ, and a constant packet transmission slot of $\tau_p = 1$ ms is set to avoid difficulties with collisions in multi-device communications [21]. These values are consistent

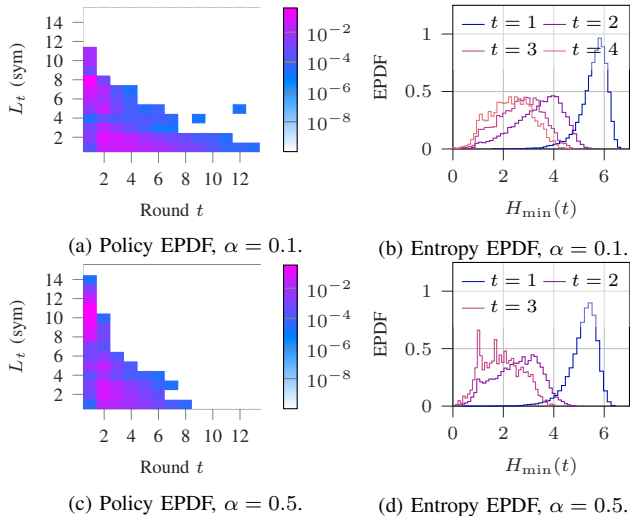


Fig. 2. Colormaps showing the EPDF of chosen actions (left) and H_{\min} (right) with RAF for $L_p = 1$ and $\gamma_{\text{DQN}} = 0.5$.

with empirical measurements for LoRa deployments [16]. All parameters for the DQN architecture and training, as well as the simulation scenario, are given in Table I.

Given the transmission protocol specification L_p , the hardware specification α , and the desired energy-latency trade-off through the exponential discount factor γ , we can optimize hyperparameters for the baseline policies and RAF.

Consider the optimization of the baseline policies by grid search: For the D-HARQ and TA policies, the only parameter is H_{th} while for the static policies the parameters are $L_t \in \mathcal{A}$ for $t = 1, \dots, T_{\text{max}} - 1$. To make a grid search feasible, the sequence L_t is defined in terms of a single parameter $L_{\text{static}} \in \{1, \dots, L_0\}$ as $L_t = L_{\text{static}}$ if $t = 1$, $L_t = L_{\text{static}} \forall t > 1$ if $1 \leq L_{\text{static}} \leq 2$, $L_t = 2, \forall t > 1$ if $2 < L_{\text{static}} \leq 10$ and $L_t = 4, \forall t > 1$ if $L_{\text{static}} > 10$. This definition is motivated by empirical results indicating that the optimal policy is tapered.

A. Adaptivity of RAF

Fig. 2 provides intuition for the choices made by the RAF scheme. The figures on the left depict the empirical probability density function (EPDF) of the chosen actions. We can notice that the strategy is generally tapered, i.e., more symbols are retransmitted in the first few rounds, and that higher values of α correspond to fewer retransmitted symbols per round and more rounds. The figures on the right show the EPDF of the minimum entropy among the transmitted symbols in the first few rounds, i.e., the optimal entropy threshold, denoted $H_{\min}(t)$. Interestingly, the entropy distribution changes significantly from the first to the second round, but only slightly in subsequent rounds: this is due to the limited amount of information delivered in shorter retransmitted packets. Finally, we note that the distribution of the minimum entropy among the transmitted symbols has a high variance. The optimal action is then hard to capture with a fixed threshold, making the TA policy highly suboptimal.

TABLE II
COMPARISON OF RAF WITH THE BASELINE METHODS

Scheme	$\mathbb{E}[T]$ (ms)			$\mathbb{E}[E_b(T)]$ (bits/mJ)			$\mathbb{E}[\mathbb{1}[\hat{c} \neq c]] \cdot 10^4$		
	$\alpha=0.1$	$\alpha=0.5$	$\alpha=0.9$	$\alpha=0.1$	$\alpha=0.5$	$\alpha=0.9$	$\alpha=0.1$	$\alpha=0.5$	$\alpha=0.9$
HARQ	1.63	1.63	1.44	36.12	34.67	33.12	1.79	1.79	1.24
D-HARQ	1.80	1.55	1.38	35.63	33.79	32.38	1.61	1.00	0.79
ST	1.59	1.59	1.19	35.90	33.42	30.89	0.97	0.97	0.39
TA	1.73	1.50	1.35	35.40	32.59	30.58	0.70	0.45	0.61
RAF	1.56	1.39	1.39	36.38	33.58	31.65	0.43	0.31	0.31

B. Comparison of Optimized Policies

Let us consider the performance of RAF when $L_p = 1$, trained with different values of α : Table II shows the average performance for the various policies in terms of latency, successful bits per mJ, and undetected error rate (UDER), with boldface indicating the best value in each column. For each policy, $\mathbb{E}[E_b(T)\gamma^T]$ with $\gamma = 0.92$ is maximized according to the respective parameters: L_{static} , H_{th} , and γ_{DQN} .

We observe from Table II that TA has the lowest number of successfully transmitted bits per energy unit, and while ST has a slightly lower latency than HARQ, the cost of rich feedback makes HARQ the preferred baseline. Looking at the UDER, we note that HARQ and D-HARQ tend to have more undetected errors than their RB-HARQ counterparts in ST and TA, and overall RAF has the lowest UDER. This highlights another advantage of RAF: retransmitting the highest-entropy symbols can steer the BP decoder towards the right codeword, reducing undetected errors.

When $\alpha = 0.1$, RAF is the most energy efficient policy while having a lower latency than the static baselines resulting in the best performance for the energy efficiency-latency trade-off. When comparing RAF with HARQ with $\alpha = 0.1$, we are able to reduce the error rate by a factor four, while also reducing the latency by 3.8 percent and increasing the energy efficiency by 0.71 percent. However, for higher α -values, the cost of feedback outweighs the benefits of RAF.

C. Pareto Dominance of RAF

We compare RAF to the baselines in the latency and energy-efficiency trade-off using the *Pareto frontier* for $\alpha = 0.1$, as RAF targets scenarios when receiving feedback consumes much less energy than transmitting. For this comparison, different hyperparameter settings are tested: $L_{\text{static}} = 1, 2, \dots, 15$ for HARQ and ST, $H_{\text{th}} = 2.9, 3.1, \dots, 7.1$ for D-HARQ and TA, and $\gamma_{\text{DQN}} = 0.1, 0.2, \dots, 0.9$, $\alpha = 0.1, 0.5$, and $L_p = 1, 2$ for RAF.

Figs. 3a and 3b depict the Pareto frontiers when $\alpha = 0.1$ and $L_p = 1, 2$ for the average number of successfully transmitted bits per energy unit versus the average latency (in ms). These results show that RAF Pareto dominates the baselines for both preamble lengths, achieving a lower latency for the same energy efficiency (or, conversely, a higher energy efficiency with the same latency). We show now that RAF can adapt to different modulation schemes by considering QPSK modulation. To be comparable with the 256-QAM modulation, an order 256 GF value is mapped to four QPSK symbols, each with normalized energy, and the SNR is lowered to -3 dB.

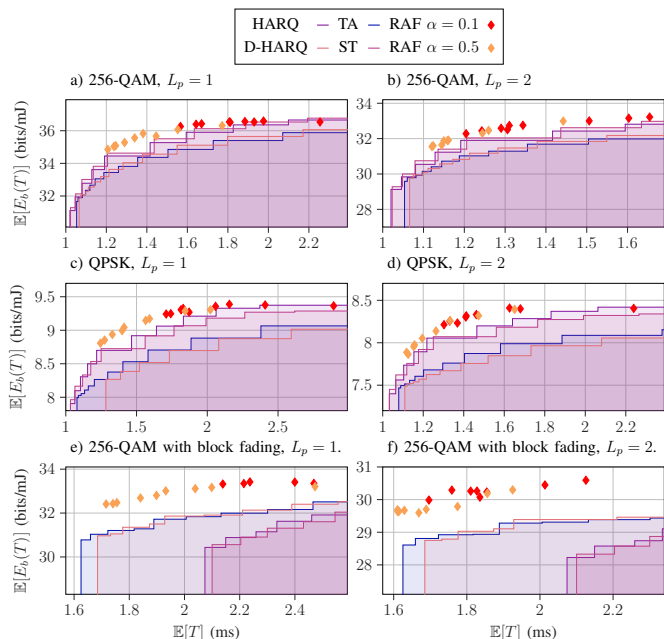


Fig. 3. Pareto frontiers for the average successful bits per mJ versus the average latency in ms for the different baselines and the RAF model when $\alpha = 0.1$ and $L_p = 1, 2$.

The results are shown in Figs. 3c and 3d: the RAF model can adapt to the modulation scheme, yielding Pareto dominant results for both of the considered modulation schemes.

Finally, we show that RAF can generalize to other channel by consider the block fading channel $\beta_t \stackrel{iid}{\sim} \mathcal{CN}(0, 1)$. The instantaneous SNR is then $\text{SNR}_t = \frac{|\beta_t|^2}{\sigma^2}$, with a mean SNR set to 6 dB. In these experiments, the RAF models trained on the AWGN channel are used for testing over the fading channel. The Pareto frontiers are seen in Figs. 3e and 3f. We can draw two conclusions from these figures: firstly, the static policies cannot adapt to a fading channel since the decisions made by the agents are independent of the instantaneous channel; hence, the D-HARQ and TA policies are the best baseline policies, while, the RAF model can generalize to a fading channel maintaining its Pareto dominance. In particular, for a latency of 2 ms, improvements of 3.9 and 3.6 percent over the optimized baselines is observed for the case of $L_p = 1$ and $L_p = 2$, respectively. An improvement by nearly 4 percent in energy-efficiency for a battery-powered IoT device can have significant implications. If for instance the expected lifetime of the battery is 10 years with the baseline, RAF increases the lifetime by nearly 5 months.

V. CONCLUSIONS AND FUTURE WORK

In this work, we introduced RAF, a DQN-based approach that enhances HARQ performance for energy-conscious devices in short-packet transmission. By shifting the complexity of adaptive HARQ to the receiver side, the transmitter only needs to decode rich feedback and retransmit the requested symbols. We considered different relative costs for transmitting and receiving feedback, and showed that RAF with a relatively high feedback cost achieves Pareto dominant policies

in the energy efficiency-latency trade-off while having a lower risk of undetected errors. This was observed for both 256-QAM and QPSK over AWGN and block fading channels.

Future work will explore more complex channels whose statistics can be learned and exploited by the receiver to further optimize the HARQ process. Moreover, it will be interesting to explore scenarios with imperfect SNR estimation, other channel codes, and feedback reception errors.

REFERENCES

- [1] F. Zhou and Y. Chai, "Near-sensor and in-sensor computing," *Nat. Electron.*, vol. 3, no. 11, pp. 664–671, 2020.
- [2] F. Guo, F. R. Yu, H. Zhang, X. Li, H. Ji, and V. C. M. Leung, "Enabling massive IoT toward 6G: A comprehensive survey," *IEEE Internet Things J.*, vol. 8, no. 15, pp. 11 891–11 915, 2021.
- [3] R. K. Singh, P. P. Puluckul, R. Berkvens, and M. Weyn, "Energy consumption analysis of LPWAN technologies and lifetime estimation for IoT application," *Sensors*, vol. 20, no. 17, p. 4794, 2020.
- [4] K. Mekki, E. Bajic, F. Chaxel, and F. Meyer, "A comparative study of LPWAN technologies for large-scale IoT deployment," *ICT Express*, vol. 5, no. 1, 2019.
- [5] A. Ahmed, A. Al-Dweik, Y. Iraqi, H. Mukhtar, M. Naeem, and E. Hossain, "Hybrid automatic repeat request (HARQ) in wireless communications systems and standards: A contemporary survey," *IEEE Commun. Surv. Tutor.*, vol. 23, no. 4, pp. 2711–2752, 2021.
- [6] A. Avranas, M. Kountouris, and P. Ciblat, "Energy-latency tradeoff in ultra-reliable low-latency communication with retransmissions," *IEEE J. Sel. Areas Commun. (JSAC)*, vol. 36, no. 11, pp. 2475–2485, 2018.
- [7] P. Andres-Maldonado, M. Lauridsen, P. Ameigeiras, and J. M. Lopez-Soler, "Analytical modeling and experimental validation of NB-IoT device energy consumption," *IEEE Internet Things J.*, vol. 6, no. 3, pp. 5691–5701, 2019.
- [8] F. Li, H. Yao, J. Du, C. Jiang, and F. R. Yu, "Green communication and computation offloading in ultra-dense networks," in *Proc. IEEE Global Telecommun. Conf. (GLOBECOM)*, 2019.
- [9] J. M. Shea, "Reliability-based hybrid ARQ," *Electronics Letters*, vol. 38, pp. 644–645(1), June 2002.
- [10] H. Yuan and P.-Y. Kam, "The LLR metric for q-ary LDPC codes with MPSK modulation over rayleigh channels with imperfect CSI," *IEEE Trans. Commun.*, vol. 60, no. 7, pp. 1793–1799, 2012.
- [11] M. Davey and D. MacKay, "Low density parity check codes over GF(q)," *IEEE Commun. Lett.*, vol. 2, no. 6, pp. 70–71, 1998.
- [12] G. Durisi, G. Liva, and Y. Polyanskiy, "Short-Packet Transmission," in *Information Theoretic Perspectives on 5G Systems and Beyond*. Cambridge Univ. Press, 2020.
- [13] R. S. Sutton and A. G. Barto, *Reinforcement Learning: An Introduction*. A Bradford Book, 2018.
- [14] V. Mnih *et al.*, "Human-level control through deep reinforcement learning," *Nature*, vol. 518, no. 7540, pp. 529–533, 2015.
- [15] L. Baird, "Residual algorithms: Reinforcement learning with function approximation," in *Mach. Learn. Proc.*, A. Prieditis and S. Russell, Eds. Morgan Kaufmann, 1995, pp. 30–37.
- [16] T. Bouguera, J.-F. Diouris, J.-J. Chaillout, R. Jaouadi, and G. Andrieux, "Energy consumption model for sensor nodes based on LoRa and LoRaWAN," *Sensors*, vol. 18, no. 7, p. 2104, 2018.
- [17] K. Kasai, D. Declercq, C. Poulliat, and K. Sakaniwa, "Multiplicatively repeated nonbinary LDPC codes," *IEEE Trans. Inf. Theory*, vol. 57, no. 10, pp. 6788–6795, 2011.
- [18] P. K. Singya, P. Shaik, N. Kumar, V. Bhatia, and M.-S. Alouini, "A survey on higher-order QAM constellations: Technical challenges, recent advances, and future trends," *IEEE Open J. Commun. Soc.*, vol. 2, pp. 617–655, 2021.
- [19] E. Visotsky, Y. Sun, V. Tripathi, M. Honig, and R. Peterson, "Reliability-based incremental redundancy with convolutional codes," *IEEE Trans. Commun.*, vol. 53, no. 6, pp. 987–997, 2005.
- [20] A. Roongta and J. M. Shea, "Reliability-based hybrid ARQ using convolutional codes," in *Proc. IEEE Int. Conf. Commun.*, vol. 4, 2003, pp. 2889–2893 vol.4.
- [21] L. Szczecinski, S. R. Khosravirad *et al.*, "Rate allocation and adaptation for incremental redundancy truncated HARQ," *IEEE Trans. Commun.*, vol. 61, no. 6, pp. 2580–2590, 2013.